

Light-Induced Stark Effect and Reversible Photoluminescence Quenching in Inorganic Perovskite Nanocrystals

Nathan D. Cottam, Chengxi Zhang, Joni L. Wildman, Amalia Patanè, Lyudmila Turyanska,* and Oleg Makarovskiy

Inorganic perovskite nanocrystals (NCs) have demonstrated a number of unique optical and electronic properties for optoelectronic applications. However, the physical properties of these nanostructures, such as the dynamics of charge carriers on different timescales and their effect on the optical recombination of carriers, are not yet fully understood. This work reports on a slow (>1 s) reversible quenching of the NC photoluminescence due to a light-induced Stark effect involving defects on the surface of the NCs and the redistribution of photoexcited carriers onto the NC surface. This phenomenon can influence the operation of optoelectronic devices based on these NCs, including hybrid photosensors based on graphene decorated with inorganic perovskite NCs, revealing their prospects and limitations.

1. Introduction

Inorganic perovskite nanocrystals (NCs) have attracted considerable attention due to their high optical quantum yield (QY), optical spectrum tunable from the visible to the UV range, and enhanced stability compared to organic based NCs.^[1–5] Integration of these NCs into novel 2D heterostructures based on graphene^[6–8] and other van der Waals materials^[9] has enabled a number of advances in optoelectronics, ranging from improved solar cells^[1,10] and LEDs^[11,12] to ultrasensitive photodetectors.^[7,8] Although recent studies revealed a similarity in the properties of perovskite NCs and other semiconductor quantum dots (QD),

such as a NC size-dependent energy gap and photoluminescence (PL) blinking or PL intermittency,^[13–15] their behavior in optoelectronic devices can be quite different^[7] and requires further investigations. This may partially arise from surface defects, typically halide vacancies, which play an important role in defining the electronic and optical properties of the NCs. Perovskite NCs are known to be highly defect tolerant due to the antibonding character of the conduction and valence bands,^[16,17] meaning that they can be optically active even with a high density of defects. However, these defects can affect the stability of the NCs and reduce their QY as they

can act as non-radiative recombination centers for photoexcited charge carriers. Organic capping ligands are widely used to passivate these surface defects, and enhance the QY and long-term stability of the perovskites, which remains one of the main challenges preventing the commercialization of these materials.^[16,18]

Here we focus on perovskite NCs based on CsPbX₃ (X = I, Br, or mix). Optical spectroscopy has been widely used for their studies, including time resolved PL (TRPL), which reveals PL lifetimes for CsPbX₃ NCs of the order of a few nanoseconds.^[4,19] On the other hand, a slower dynamic has been reported in long-term (days to months) PL stability studies, assessing PL properties under different environmental storage conditions, as an indicator of the shelf-life of the NCs.^[2,12] More recently, studies of the CsPbX₃ PL and its time dependence also revealed an irreversible high temperature and/or high laser power bleaching and photodegradation^[13,19] or partially reversible light-induced ion migration.^[20–23]

In this paper we report on a slow (>1 s), reversible red shift and quenching of the PL emission of CsPbX₃ NCs due to a light-induced Stark effect involving the transfer of photoexcited charges on the surface of the NCs. Our experimental findings are in good agreement with a simple theoretical model based on a triangular quantum confinement potential for the photogenerated charges. The light-induced Stark effect described here can explain the slow response time and reversible dynamics of photoexcited charges previously reported in perovskite NCs/graphene photon detectors.^[7] Here, we demonstrate a similarity between the temporal response of the NC PL intensity and the photoconductivity of single layer graphene decorated with the NCs. This enables us to correlate the charge transfer at the graphene/NCs interface and the figures of merit of these hybrid photodetectors, such as their high photoresponsivity and slow response time.

N. D. Cottam, Dr. C. Zhang, Prof. A. Patanè, Dr. O. Makarovskiy
School of Physics and Astronomy
University of Nottingham
Nottingham NG7 2RD, UK

Dr. C. Zhang
Key Laboratory of Advanced Display and System Applications
Shanghai University
149 Yanchang Road, Shanghai 200072, China

J. L. Wildman, Dr. L. Turyanska
Faculty of Engineering
University of Nottingham
Nottingham NG7 2RD, UK
E-mail: Lyudmila.Turyanska@nottingham.ac.uk

 The ORCID identification number(s) for the author(s) of this article can be found under <https://doi.org/10.1002/adom.202100104>.

© 2021 The Authors. Advanced Optical Materials published by Wiley-VCH GmbH. This is an open access article under the terms of the Creative Commons Attribution License, which permits use, distribution and reproduction in any medium, provided the original work is properly cited.

DOI: 10.1002/adom.202100104

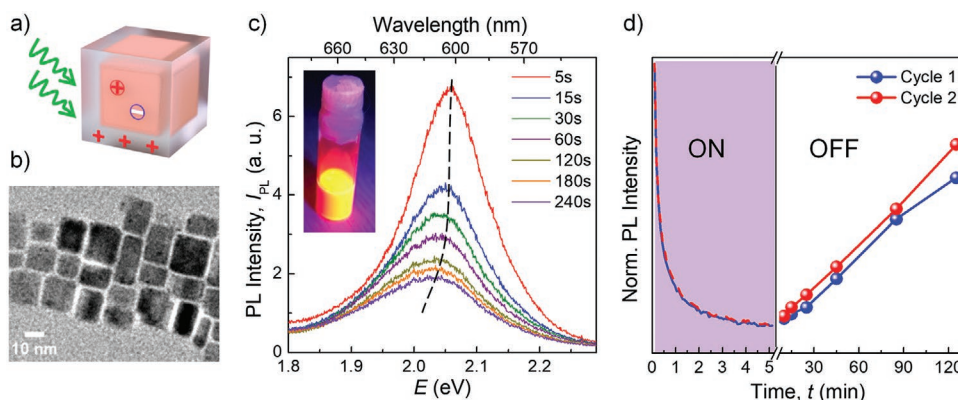


Figure 1. a) Sketch of a photoexcited electron and hole pair and positively charged surface defects on a perovskite NC. b) A representative TEM image of CsPb(Br:I = 2:3)₃ perovskites NCs. c) Room temperature PL spectra recorded at different times during sample exposure to laser light ($\lambda = 532$ nm, $P = 2 \mu\text{W}$). The dashed line follows the evolution of the PL peak over time. Inset: optical image of CsPb(Br:I)₃ NCs in solution. d) Quenching of the PL intensity under continuous excitation power ($P = 2 \mu\text{W}$, exposure time $t < 5$ min) and its recovery, as probed by short laser pulses (5 s-long pulses, $P = 2 \mu\text{W}$, and $t > 5$ min).

2. Optical Studies of Perovskite NCs

In this work we used inorganic CsPbX₃ perovskite NCs with cubic-shape and average size of $l = 14 \pm 3$ nm (Figure 1a,b), as measured by transmission electron microscopy (TEM). A mixture of oleic acid, oleylamine, and iminodibenzoic acid is used to cap the NCs, providing high stability and durability of the NCs. It is generally accepted that the strength of ligand binding and the quality of surface passivation define the QY and optical stability of the NCs. Capping ligands are used to passivate dangling bonds and defects on the NC surface, which are known to act as trap states for charge carriers.^[24,25]

The band edge optical emission of these NCs can be tuned by the halogen content from 520 nm for CsPbBr₃ to 680 nm for CsPbI₃. In contrast, it is not very sensitive to the NC size, which is larger than the exciton Bohr radius ($r_B = 3.6$ nm for CsPbBr₃ and $r_B = 6$ nm for CsPbI₃).^[4,12] The large exciton binding energy of the perovskite NCs ($E_B > 50$ meV)^[26,27] and linear dependence of the PL emission intensity on the excitation power suggest an excitonic emission even at room temperature. For the NC films, upon initial exposure to focused continuous laser light ($\lambda = 532$ nm, $P < 2$ mW, laser spot diameter $\approx 5 \mu\text{m}$), we observe a slow exponential decay of the PL intensity over time (Figure 1c,d), with a characteristic decay time τ_1 of several seconds that depends on the optical power. We also observe a second, slower temporal decay of the signal with a relaxation time $\tau_2 > \tau_1$ (see details of the bi-exponential fit to the PL decay in SI1, Supporting Information). The observed PL decay is reversible, although the recovery time is significantly slower (≈ 2 h) (Figure 1d).

The energy peak position and full width at half maximum (FWHM) of the PL emission at short times ($t < 10$ s) are the same for all studied laser powers, $20 \text{ nW} < P < 200 \mu\text{W}$ (see SI1, Supporting Information). However, the time evolution of the PL is power dependent and more pronounced for exposure to high laser powers (Figure 2a). The PL decay time, τ_1 , decreases with increasing laser power (inset in Figure 2a). The observed evolution of the PL intensity is accompanied by a time-dependent red shift of the PL peak position, ΔE_{PL} , (Figure 2b) and broadening

of the FWHM (Figure 2c). Thus, under continuous laser excitation of the NCs, the intensity, FWHM, and peak position of the PL emission change over time and the temporal dynamics become faster with increasing laser power. For example, $\tau_1 \approx 5.4$ s, $\Delta E_{\text{PL}} \approx 50$ meV, and $\text{FWHM} \approx 60$ meV are measured for $P = 200 \mu\text{W}$, compared to $\tau_1 > 100$ s, $\Delta E_{\text{PL}} < 10$ meV, and $\text{FWHM} \approx 10$ meV for $P = 0.02 \mu\text{W}$. We note that these changes are fully reversible over several cycles of ON/OFF illumination (Figure 2d–f) and we observe fully restored PL intensity, peak position, and FWHM.

The photo-induced time-dependent evolution of the PL signal is affected by temperature and becomes more pronounced at $T > 100$ K (Figure 3a–c). At $T < 100$ K we do not observe any noticeable time-dependent change of PL intensity (Figure 3a), peak position (Figure 3b) or FWHM (Figure 3c). The T -dependence of the PL peak position depends on the laser exposure time: for $t < 10$ s, a blue shift of E_{PL} is observed with increasing T ; in contrast, for $t = 120$ s a red shift is observed (inset in Figure 3a). In these studies, a low laser power ($P \approx 2.5 \text{ W mm}^{-2}$) is used to avoid irreversible changes of the perovskite crystal structures previously reported for exposure to higher laser powers.^[13,19,23] We exclude a laser heating effect in our studies, as this should cause a blue shift of the PL emission,^[28,30] rather than the red shift reported here. Furthermore, the observed strong quenching of PL intensity cannot be explained by laser heating as for temperatures in the range 250 to 350 K, our studies and those from the literature^[28,30] indicate only relatively small changes in PL intensity.

A blue shift of E_{PL} with increasing temperature can arise from the interplay between the electron-phonon renormalization and thermal lattice expansion. These tend to have opposite effects on the bandgap energy of CsPbX₃ NCs causing a blue shift of PL with increasing temperature.^[28,29] A different, more complex scenario is observed in our temperature dependent optical experiments, requiring additional effects to be considered. At $T > 150$ K, the optical properties are influenced by both temperature and time dependent phenomena. When $\Delta E_{\text{PL}}(t) > \Delta E_{\text{PL}}(T)$, a red shift of E_{PL} is observed (Figure 3b). This is suggestive of a light-induced Stark effect

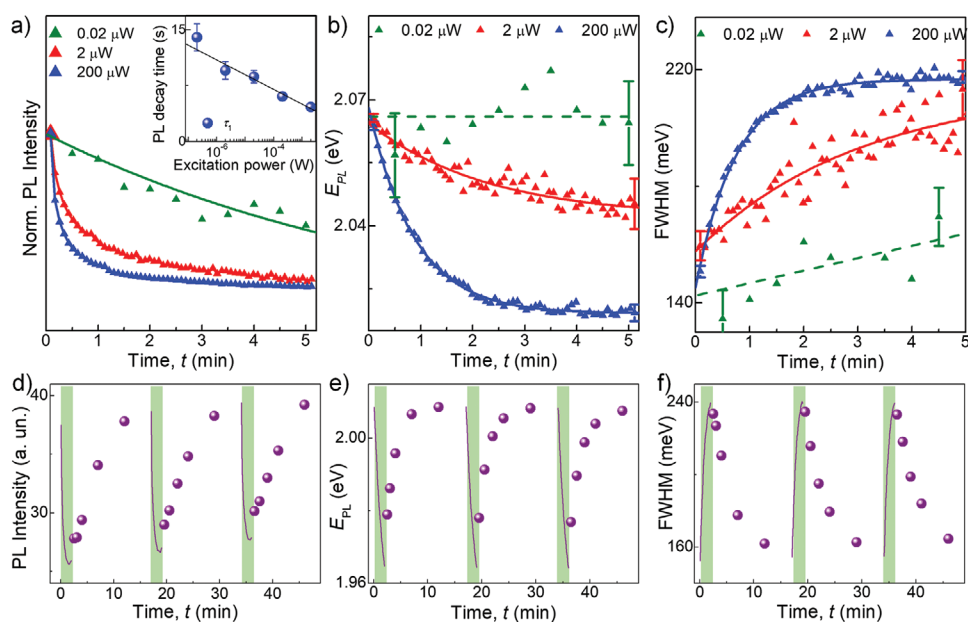


Figure 2. a) Room temperature PL intensity for CsPb(Br:I)₃ NCs versus time for different excitation powers ($\lambda = 532$ nm). Inset: decay times, τ_1 , versus power, as estimated using a bi-exponential fit of the data in the main figure. The line is a guide to the eye. b) PL peak position, E_{PL} , and c) FWHM versus time for continuous exposure of the NCs to laser light at three different powers ($\lambda = 532$ nm). Lines are guides to the eye. d–f) Time-dependence of the PL intensity, PL peak position (E_{PL}), and FWHM during three ON (line)/OFF (spheres) cycles of light exposure. Measurements were performed at room temperature with excitation power $P \approx 0.3 \mu\text{W}$ at $\lambda = 532$ nm.

and a trap-assisted recombination of carriers, as discussed in greater detail below. We note that the t -dependent change of the PL peak position and intensity are accompanied by a PL broadening (Figure 3c). This can arise from inhomogeneity of charge distribution and charging/discharging times for the NCs in the ensemble (see S12 and S13, Supporting Information).

In summary, our temporal and temperature dependent study of the PL signal reveal photo-induced effects that can arise from: i) the T -dependence of the band gap;^[19] ii) a T -dependence of charge trapping; and iii) a light-induced Stark effect.

In order to investigate the origin of the photoinduced time-dependent red shift of E_{PL} , we examine the power dependence of the PL temporal dynamics (Figure 4a). By taking a snapshot of the PL intensity versus power at different times, we deter-

mine the power-dependence of the PL intensity (I_{PL}) at a given time. As shown in Figure 4b for $t = 15$ s, I_{PL} follows a power law, $I_{PL} \approx P^\alpha$, where $\alpha = 0.5$. The value of α varies from ≈ 0.5 at $t = 15$ s to ≈ 0.6 at $t = 300$ s (inset of Figure 4b). Thus, the dependence of the PL intensity on power becomes stronger for a longer exposure of the NC to light.

To investigate further this effect, we use graphene field effect transistor (FET) devices decorated with a layer of perovskite NCs.^[7,31] Interestingly, we find that the power dependence of the photocurrent (I_{ph}) of these devices is similar to that observed in the optical studies. The photocurrent depends on power as $I_{ph} \approx P^\beta$, leading to a P -dependent photoresponsivity $R = I_{ph}/P \sim P^{\beta-1} \sim P^{-0.6}$ and $\beta \approx 0.4$ (Figure 4c). We ascribe these sublinear power dependences of I_{PL} and I_{ph} to the contribution of defects on the NC surface.^[7]

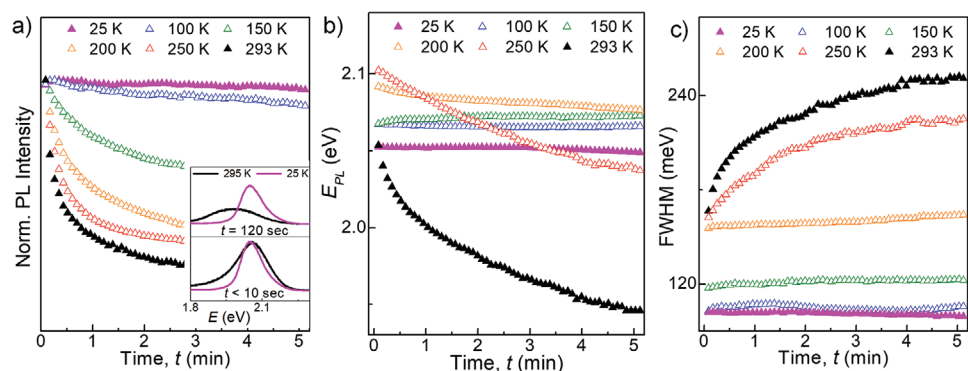


Figure 3. Temporal evolution of the a) normalized intensity, b) peak position, and c) FWHM of the PL spectra of CsPb(Br:I)₃ NCs under continuous illumination ($\lambda = 532$ nm, $P = 2$ mW) at different temperatures. Inset: PL spectra before and after 2 min of continuous illumination ($\lambda = 532$ nm, $P = 2$ mW) of CsPb(Br:I)₃ NCs at $T = 25$ K and $T = 293$ K.

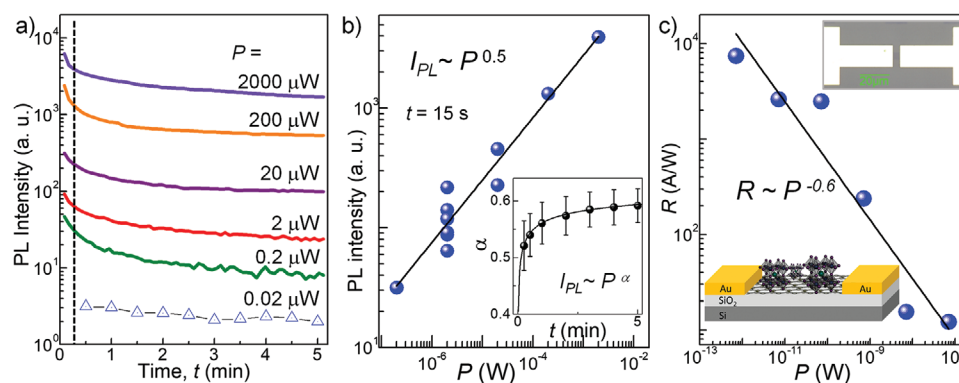


Figure 4. a) Dependence of the PL intensity (I_{PL}) of CsPb(Br:I)₃ NCs on laser exposure time ($\lambda = 532$ nm) for different excitation powers at room temperature. b) PL intensity as a function of power at $t = 15$ s (marked by a vertical line in (a)) fitted by $I_{PL} \approx P^\alpha$ with $\alpha = 0.5$. Inset: a graph showing the evolution of the coefficient α with increasing exposure time. c) Photoresponsivity (R) as a function of power, P ($\lambda = 405$ nm) and its fit by $R \approx P^{-0.6}$ for CsPb(Br:I)₃ NCs deposited on a graphene field effect transistor (FET). (Insets) Schematic of the device and optical image of a commercial graphene FET.^[32]

Electrical measurements of our perovskite/graphene FETs demonstrate that CsPbX₃ NCs on graphene act as donors, transferring electrons into the graphene layer, hence the NCs become positively charged. This doping effect may arise from the ionization of deep (≈ 0.3 eV) defect levels, likely associated with Pb-atoms on the NC surface.^[7] In these devices, the time-dependence of the photocurrent is slow with a long relaxation time of ≈ 100 s, which is comparable to that observed in the PL decay reported here (Figures 2 and 3). Furthermore, the transfer of photo-created electrons from the NCs onto graphene is a thermally activated process that occurs for temperatures $T > 200$ K. This is ascribed to the thermal ionization of charged traps on the surface of the NCs with a binding energy $E \approx 0.3$ eV.^[7] Thus, the reversible slow PL quenching reported in this work and the previously observed quenching of the photocurrent in CsPbX₃/graphene FET devices can arise from the same phenomenon, which is a temperature- and time-dependent charging/discharging of the NCs via surface traps. The defect-assisted high photoresponsivity ($R \approx 10^6$ A W⁻¹) in graphene transistors decorated with the NCs arises from a preferential transfer of photo-created electrons from the NCs into graphene. This is accompanied by a giant hysteresis of the graphene resistance that is dependent on electrostatic gating, light, and temperature.^[7] The positive charge on the surface of the NCs also influences the PL emission, as described in the following section.

3. Modeling the Light-Induced Stark Effect

We assign the reversible decay of the PL intensity to non-radiative recombination of carriers that are trapped onto surface defects of the CsPbX₃ NCs. Our experimental results indicate that more than one charge is trapped on the NC surface, resulting in the separation of photocreated electron-hole pairs within the NCs, which overall remain neutral. The efficiency of the non-radiative recombination at the surface of a perovskite NC can be significantly enhanced by a photo-generated internal electric field, which acts to spatially separate photoexcited electrons and holes in the NC, pulling electrons toward the surface (inset in Figure 5a and SI2, Supporting Information). We model

the effect of this surface charge and corresponding electric field by an infinite triangular quantum well (TQW) model.^[33]

The confinement potential of carriers in the NC is affected by the electrostatic potential generated by surface charges (black line in Figure 5a) and the quantization of motion due to the formation of TQW (dashed blue line in Figure 5a). Here, we assume that the energy of the photoexcited holes in the valence band is not affected by surface charges as they have a larger effective mass than electrons (inset in Figure 5a). This simple model can be used to estimate the number of charges, N_e , on the surface of the NC required to achieve the measured red shift of the NC PL emission (Figure 5b and SI2, Supporting Information). In this model we assume that all photoexcited surface charges are uniformly distributed on one side of the perovskite NC. We note that different spatial configurations of surface charges and their spread to other sides of the NC can affect the confinement potential, leading to relatively small changes in the estimated energy red shift (see SI3, Supporting Information). We note that in these measurements of the NC ensemble, we do not observe charge related phenomena associated with individual NCs, for example, blinking and single photon emission and relevant photon antibunching.^[34] The full recovery of the PL properties observed in our work is well explained by the separation of charges leading to a Stark effect.

Informed by our previous photocurrent studies on similar CsPbX₃ NCs,^[7] we assume that the surface traps are positively charged and consider classical electrostatics (black line in Figure 5a,b) and the quantum confinement of an electron in the electrostatic potential (blue line in Figure 5a,b). Figure 5c shows the calculated PL shift ΔE_{PL} as a function of the number of surface charges N_e . From our model we estimate that 5 charges located on the single side of a cubic CsPbX₃ NC are sufficient to account for the measured red shift $\Delta E_{PL} \approx 50$ meV (red line in Figure 5b). From the energy potential of Figure 5a, we estimate that the corresponding electric field is $E = 2 \times 10^7$ V m⁻¹.

In Figure 5c we model the time-dependent charging of the NC surface to show the relationship between the red shift and the number of surface charges, N_e , which aligns well with the experimental data (Figure 2b). This dependence describes the surface charging process where the number of trapped charges change with time as:

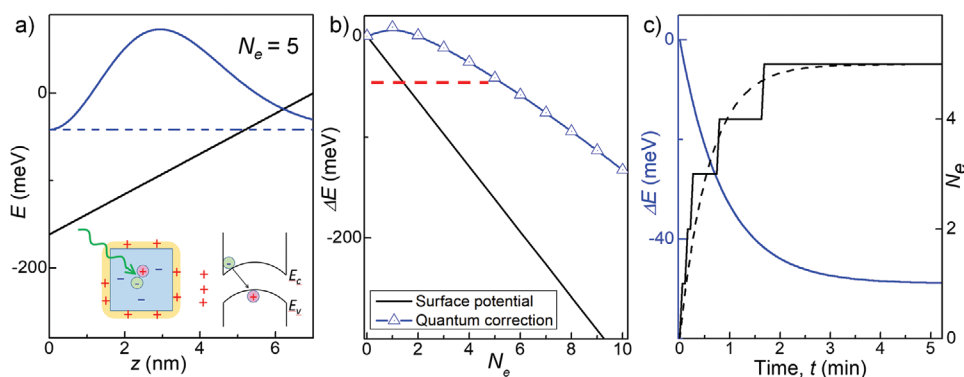


Figure 5. a) Schematic of photoexcited charges in a perovskite NC under light, showing electrons being pulled on the surface of the NC due to positively charged surface defects (inset) and spatial profile (black line) of the potential in the NC due to surface charges ($N_e = 5$ elementary charges per NC). z is the distance from the surface to the center of the NC. The average size of the NCs is ≈ 14 nm. Dashed and solid blue lines represent, respectively, the electron ground state energy and its wave function in TQW. b) Electrostatic potential energy on the surface of the NC (black line) and relevant electron ground state energy calculated using a TQW model (blue line) for different number of surface charges, N_e . The dashed red line shows the measured PL red shift. c) Model of the red shift (blue line) over time assuming a charging time constant of 35 s. The solid and dashed black lines represent relevant number of surface charges; steps on the solid line represent the quantization of the number of surface charges, N_e .

$$N_e = N_e^{\max} (1 - \exp(-t/\tau_c)) \quad (1)$$

where N_e^{\max} is the maximum number of surface charges ($N_e = N_e^{\max}$ at $t = \infty$), t is the exposure time, and τ_c is a characteristic charging time. Note that N_e^{\max} and τ_c are dependent on the laser power (see Figure 2 for corresponding experimental data). Our results suggest that the light-induced Stark effect in the NCs can account for both the red shift and reversible time decay of the PL intensity. The slow dynamics of the PL intensity indicates that the trapping/de-trapping of charges on the NC surface is a process that takes several seconds–minutes, a time-scale different from the fast (nanoseconds) dynamics of photo-excited carriers in bulk and NCs based on CsPbI_3 ^[4,19] or very slow (days) dynamics associated with degradation processes.^[2,12]

4. Discussion

Slow dynamic processes in semiconductor NCs are typically associated with deep surface traps. These are responsible for a number of quantum phenomena such as QD blinking. Blinking (or PL intermittency) is a well-known phenomenon in colloidal QDs and it is also related to non-radiative recombination of carriers on surface charge traps.^[35] Recent findings of a similar blinking effect in inorganic perovskite NCs^[36] demonstrate a similarity between colloidal QDs and perovskite NCs, underlining the importance of quantum confinement effects for the understanding of the optical response in these systems.^[13,36] Interestingly, an electrically induced Stark effect was recently reported in CsPbX_3 NCs, where it was also accompanied by a PL quench and explained using the electric field dependence of the PL intermittency (blinking) effect.^[15] The efficiency of the non-radiative recombination at the surface of a perovskite NC can be significantly enhanced by a photo-generated internal electric field, which can spatially separate photo-excited electrons and holes in the NC and attract one of them toward the surface (Figure 4a), as shown here. This process

leads to the trapping of one type of carrier on the surface of perovskite NCs and can strongly affect the performance of optoelectronic devices based on graphene.^[7,8] Also, charged defects on the surface of the NCs can affect the photovoltage generated in perovskite-based solar cells.^[10]

Beside surface-related effects, a slow photoresponse can also be caused by bulk properties. For example, another mechanism that could lead to a reversible PL quench under intensive light exposure is light-induced segregation of iodine- and bromine-rich regions in the bulk of mixed halide perovskites and migration of iodine ions.^[20–23] Manifestations of this effect are rather random: a long (minutes) light exposure can lead to a PL intensity decrease,^[22,23] increase^[21] or decrease of one and increase of the other PL peaks.^[20] Photodegradation of individual NCs has also been reported: it manifests through an irreversible blue shift and quenching of the PL emission ascribed to a photo-accelerated reaction.^[37] Photoinduced iodine ion migration is usually observed in CsPbX_3 NCs^[38] and films, and is associated with a red shift of the PL peak.^[22,23] Reversible migration of iodine ions has not been found in individual perovskite NCs.^[23] The reversibility of optical properties observed in our work (Figure 2d–f) allows to exclude an ion migration effect. The Stark effect model explains our experimental results, excluding photobleaching, photodegradation and ion migration effects, which lead to irreversible or partially reversible properties. Our data indicate a light-induced reversible charge accumulation on the surface of the NCs that does not cause a permanent degradation of the PL emission. This is caused by the presence of defects and charge trapping over a time scale longer than the time for migration of photo-created electrons toward the surface, resulting in a slow temporal dynamic of the PL emission. As the defect forms and electrons accumulate on the surface, the internal electric field increases, causing a gradual red shift of the PL emission with time. Our simulation as well as experimental data (Figure 2) reveal the saturation of surface charge within a few minutes of exposure of the NCs to light. The saturation can arise from increasing Coulomb repulsion interactions, which prevents further accumulation of charges on the

NC surface. The small excitation power and full recovery of the PL signal in our experiments exclude the partially reversible PL observed at high laser powers in bulk crystals^[23] as well as photodegradation and bleaching effects observed at high power and/or temperature.^[13,19] To probe the effect of surface passivation on the manifestation of the Stark effect, we performed preliminary PL studies of similar NCs capped with halogen-containing capping ligands that are associated with better surface passivation.^[39] These do not reveal any noticeable photoinduced changes associated with a Stark effect, hence confirming our hypothesis. Systematic studies of the perovskite NCs synthesized with different capping ligands^[39] and core/shell NCs^[40] are needed to further explore this phenomenon.

5. Conclusion

We have experimentally studied the dynamics of photoexcited charges in inorganic halide CsPbX₃ NCs. We have shown that the slow (minutes) formation of positive charges on the surface of the NCs significantly affect the NC optical response. We ascribe this behavior to a photoinduced time-dependent Stark effect. This can be described using a simple quantum mechanical model of the confined energy states of a CsPbX₃ NC under a light-induced electric field. We emphasize that the presented effect is fully reversible and recoverable. Thus, it is different from the previously reported ion migration and other bulk effects causing irreversible or partially reversible lattice modifications. The decay of the PL signal is accompanied by the time-dependent red shift of the PL peak position and broadening of the PL spectrum. We compare these optical measurements with transport measurements on CsPbX₃/graphene heterostructures used as VIS–UV photon detectors and relay the similarity of the temporal dynamics of photo-created charges to the surface defect states on the NCs. The combined optical (PL) and transport (photocurrent) studies of photoexcited charges in 0D/2D heterostructures, such as CsPbX₃/graphene, provides a versatile tool for probing the charge dynamics in these systems. This information is essential to improve the performance of 0D/2D photodetectors, such as responsivity and response time. Thus, this study reveals unique electronic and optical properties of inorganic perovskite NCs of fundamental and technological relevance for optoelectronic applications.

6. Experimental Section

Materials: Inorganic CsPbX₃ perovskite NCs (X = I, Br, or molar ratio of Br:I = 2:3) were synthesized following the procedure reported by C. Zhang et al.^[12] and were drop-casted on different substrates for optical studies. Commercial graphene FETs (GFETs) with large (up to 35 000 μm²) surface area on a SiO₂/Si substrate were purchased from Graphenea.^[27] Following the NC deposition on a SiO₂/Si or on a graphene/SiO₂/Si substrate, the samples were dried in vacuum (≈10⁻⁶ mbar) overnight.

Optical Studies: A frequency-doubled Nd:YVO₄ laser (wavelength λ = 532 nm and power, P, in the range 20 nW–2 mW) was used for optical excitation. The laser beam was focused to a spot diameter of ≈5 μm. To control the amount of light during the laser exposure, the laser was used both in continuous wave (CW) and pulsed modes. PL spectra were recorded using a Horiba LabRAM system equipped with a Si CCD

array detector. The temporal decay of the PL signal was measured by using a CW laser excitation and recording the PL spectra at regular time intervals, typically every 5 s (i.e., 5 s integration time per spectrum). The recovery of the PL intensity was measured using a pulsed laser mode whereby the laser was switched on for the minimum time required to acquire the PL spectrum (≈5 s). Time intervals (>10 min) were used to allow for adequate recovery of the PL signal between measurements. All measurements were performed in an optical cryostat in the temperature range 10 K < T < 300 K.

Photocurrent Measurements: Commercial CVD monolayer graphene on 300 nm SiO₂/Si substrates were purchased from Graphenea.^[32] The NCs were drop-cast onto a planar graphene two-terminal device with a short channel length (≈10 μm) defined by electron beam lithography. NCs were deposited by drop-casting. Electrical and photocurrent measurements were performed in the DC mode using Keithley-2400 source-meters and Keithley-2010 multimeters. A solid-state laser (λ = 405 nm) was used for the photocurrent studies.

Supporting Information

Supporting Information is available from the Wiley Online Library or from the author.

Acknowledgements

The authors acknowledge support from the DSTL and from the Engineering and Physical Sciences Research Council [grant number EP/P031684/1]. This project has received funding from the European Union's Horizon 2020 research and innovation programme under grant agreement Graphene Core3. CZ acknowledges funding from China Postdoctoral Science Foundation Grant number 2020M680058. The authors also acknowledge Graphenea for providing graphene and the nmRC for providing access to facilities and assistance with the morphological studies.

Conflict of Interest

The authors declare no conflict of interest.

Data Availability Statement

The data that support the findings of this study are available on request from the corresponding author. The data are not publicly available due to privacy or ethical restrictions.

Keywords

charge dynamics, graphene, inorganic perovskites, photosensors, Stark effect

Received: January 18, 2021

Revised: March 16, 2021

Published online:

[1] B. Li, Y. Zhang, L. Fu, T. Yu, S. Zhou, L. Zhang, L. Yin, *Nat. Commun.* **2018**, *9*, 1076.

[2] Z. Lin, R. Huang, W. Zhang, Y. Zhang, J. Song, H. Li, D. Hou, Y. Guo, C. Song, N. Wan, P. K. Chu, *Adv. Funct. Mater.* **2018**, *28*, 1805214.

- [3] J. Lu, X. Sheng, G. Tong, Z. Yu, X. Sun, L. Yu, X. Xu, J. Wang, J. Xu, Y. Shi, K. Chen, *Adv. Mater.* **2017**, *29*, 1700400.
- [4] L. Protesescu, S. Yakunin, M. I. Bodnarchuk, F. Krieg, R. Caputo, C. H. Hendon, R. X. Yang, A. Walsh, M. V. Kovalenko, *Nano Lett.* **2015**, *15*, 3692.
- [5] C. Zhang, S. Wang, X. Li, M. Yuan, L. Turyanska, X. Yang, *Adv. Funct. Mater.* **2020**, *30*, 1910582.
- [6] V. V. Brus, F. Lang, S. Fengler, T. Dittrich, J. Rappich, N. H. Nickel, *Adv. Mater. Interfaces* **2018**, *5*, 1800826.
- [7] N. D. Cottam, C. Zhang, L. Turyanska, L. Eaves, Z. Kudrynskiy, E. E. Vdovin, A. Patanè, O. Makarovskiy, *ACS Appl. Electron. Mater.* **2020**, *2*, 147.
- [8] M. Gong, R. Sakidja, R. Goul, D. Ewing, M. Casper, A. Stramel, A. Elliot, J. Z. Wu, *ACS Nano* **2019**, *13*, 3714.
- [9] J. He, J. Su, Z. Lin, S. Zhang, Y. Qin, J. Zhang, J. Chang, Y. Hao, *J. Phys. Chem. C* **2019**, *123*, 7158.
- [10] J. Wang, J. Zhang, Y. Zhou, H. Liu, Q. Xue, X. Li, C. C. Chueh, H. L. Yip, Z. Zhu, A. K. Y. Jen, *Nat. Commun.* **2020**, *11*, 177.
- [11] M. Cao, Y. Xu, P. Li, Q. Zhong, D. Yang, Q. Zhang, *J. Mater. Chem. C* **2019**, *7*, 14412.
- [12] C. Zhang, L. Turyanska, H. Cao, L. Zhao, M. W. Fay, R. Temperton, J. O'Shea, N. R. Thomas, K. Wang, W. Luan, A. Patanè, *Nanoscale* **2019**, *11*, 13450.
- [13] Y. S. Park, S. Guo, N. S. Makarov, V. I. Klimov, *ACS Nano* **2015**, *9*, 10386.
- [14] L. Hou, C. Zhao, X. Yuan, J. Zhao, F. Krieg, P. Tamarat, M. V. Kovalenko, C. Guo, B. Lounis, *Nanoscale* **2020**, *12*, 6795.
- [15] D. K. Sharma, S. Hirata, V. Biju, M. Vacha, *ACS Nano* **2019**, *13*, 624.
- [16] H. Huang, M. I. Bodnarchuk, S. V. Kershaw, M. V. Kovalenko, A. L. Rogach, *ACS Energy Lett.* **2017**, *2*, 2071.
- [17] Q. A. Akkerman, G. Raino, M. V. Kovalenko, L. Manna, *Nat. Mater.* **2018**, *17*, 394.
- [18] X. Zheng, Y. Hou, H.-T. Sun, O. F. Mohammed, E. H. Sargent, O. M. Bakr, *J. Phys. Chem. Lett.* **2019**, *10*, 2629.
- [19] B. T. Diroll, G. Nedelcu, M. V. Kovalenko, R. D. Schaller, *Adv. Funct. Mater.* **2017**, *27*, 1606750.
- [20] C. G. Bischak, C. L. Hetherington, H. Wu, S. Aloni, D. F. Ogletree, D. T. Limmer, N. S. Ginsberg, *Nano Lett.* **2017**, *17*, 1028.
- [21] D. W. deQuilettes, W. Zhang, V. M. Burlakov, D. J. Graham, T. Leijtens, A. Osherov, V. Bulovic, H. J. Snaith, D. S. Ginger, S. D. Stranks, *Nat. Commun.* **2016**, *7*, 11683.
- [22] S. Draguta, O. Sharia, S. J. Yoon, M. C. Brennan, Y. V. Morozov, J. S. Manser, P. V. Kamat, W. F. Schneider, M. Kuno, *Nat. Commun.* **2017**, *8*, 200.
- [23] H. Zhang, X. Fu, Y. Tang, H. Wang, C. Zhang, W. W. Yu, X. Wang, Y. Zhang, M. Xiao, *Nat. Commun.* **2019**, *10*, 1088.
- [24] G. J. Wetzelaer, M. Scheepers, A. M. Sempere, C. Momblona, J. Avila, H. J. Bolink, *Adv. Mater.* **2015**, *27*, 1837.
- [25] C. Giansante, I. Infante, *J. Phys. Chem. Lett.* **2017**, *8*, 5209.
- [26] M. Baranowski, P. Plochocka, R. Su, L. Legrand, T. Barisien, F. Bernardot, Q. Xiong, C. Testelin, M. Chamarro, *Photonics Res.* **2020**, *8*, A50.
- [27] M. Baranowski, P. Plochocka, *Adv. Energy Mater.* **2020**, *10*, 1903659.
- [28] Q. Han, W. Wu, W. Liu, Q. Yang, Y. Yang, *J. Lumin.* **2018**, *198*, 350.
- [29] S. M. Lee, C. J. Moon, H. Lim, Y. Lee, M. Y. Choi, J. Bang, *J. Phys. Chem. C* **2017**, *121*, 26054.
- [30] B. T. Diroll, H. Zhou, R. D. Schaller, *Adv. Funct. Mater.* **2018**, *28*, 1800945.
- [31] J. H. Gosling, O. Makarovskiy, F. Wang, N. D. Cottam, M. T. Greenaway, A. Patanè, R. D. Wildman, C. J. Tuck, L. Turyanska, T. M. Fromhold, *Commun. Phys.* **2021**, *4*, 30.
- [32] Graphenea, *Graphenea GFET-S10 for Sensing Applications*, www.graphenea.com/products/gfet-s10-for-sensing-applications-10-mm-x-10-mm (accessed: 2020).
- [33] J. H. Davies, *The Physics of Low-dimensional Semiconductors*, Cambridge University Press, New York **1998**.
- [34] N. Yarita, T. Aharen, H. Tahara, M. Saruyama, T. Kawawaki, R. Sato, T. Teranishi, Y. Kanemitsu, *Phys. Rev. Mater.* **2018**, *2*, 116003.
- [35] A. L. Efros, D. J. Nesbitt, *Nat. Nanotechnol.* **2016**, *11*, 661.
- [36] N. A. Gibson, B. A. Koscher, A. P. Alivisatos, S. R. Leone, *J. Phys. Chem. C* **2018**, *122*, 12106.
- [37] G. Yuan, C. Ritchie, M. Ritter, S. Murphy, D. E. Gómez, P. Mulvaney, *J. Phys. Chem. C* **2018**, *122*, 13407.
- [38] I. Karimata, Y. Kobori, T. Tachikawa, *J. Phys. Chem. Lett.* **2017**, *8*, 1724.
- [39] Y. Huang, W. Luan, M. Liu, L. Turyanska, *J. Mater. Chem. C* **2020**, *8*, 2381.
- [40] C. Zhang, S. Wang, X. Li, M. Yuan, L. Turyanska, X. Yang, *Adv. Funct. Mater.* **2020**, *30*, 1910582.